JOURNAL OF MATERIALS SCIENCE 29 (1994) 6123–6130

Development of porous zirconia spheres by polymerization-induced colloid aggregation – effect of polymerization rate

M. J. ANNEN, R. KIZHAPPALI, P. W. CARR*, A. McCORMICK‡
*Department of Chemical Engineering and Material Science, and *Department of Chemistry and Institute for Advanced Studies in Bioprocess Technology, University of Minnesota, Minneapolis, MN 55455, USA*

Polymerization-induced colloid aggregation is used to synthesize spheres of narrow size distribution which are porous aggregates of ZrO_2 colloids. Variation of the reaction pH has been investigated to determine the optimum rate of polymerization of the urea–formaldehyde resin. At the optimum rate, a colloid packing structure is formed where a balance of high porosity and high strength of the aggregates is achieved. This optimum coincides with the maximum yield of the ~5 μm sintered (polymer-free) particles. Particles synthesized at pH values below the optimum are mechanically weak; some are hollow spheres. Variation of the pore structure, and thus colloid packing structure, is elucidated by nitrogen adsorption and apparent density measurements. Differences on either side of the optimum pH are related to the efficiency of polymer-bridge formation between colloids.

1. Introduction

Interest is growing in the development of porous zirconia (ZrO_2) as a column-packing material for high-performance liquid chromatography (HPLC) [1–5] because of its excellent chemical stability at high pH (> 13). We are investigating processes for the preparation of controlled-pore zirconia that would be useful as a column-packing material for the HPLC separation of proteins, for catalysis and perhaps other applications. For HPLC, the particles should be spherical and uniform in size between 5 and 10 μm in diameter, with pores ranging from 20–50 nm in diameter. A method for the synthesis of crystalline, porous zirconia through controlled crystallite agglomeration was reported by Bleier and Cannon [6]. However, the agglomerates were submicrometre in size and, based on the surface area and pore-volume data reported, the pores were smaller than 20 nm. Another promising synthesis method was reported by Iler and McQueston [5]. It involves the controlled aggregation of ZrO_2 colloids by the acid-catalysed polymerization of urea and formaldehyde in the dispersing solvent.

Controlled flocculation of colloids through the use of adsorbing polymers is well documented [7–13], and the interactions which can lead to either polymer-induced stabilization or flocculation have been summarized [8, 9]. Bridging flocculation induced by adsorbed polymer is a complicated process which depends on solvent quality, polymer concentration, molecular weight and polymer adsorption energy. The theory of Scheutjens and Fleer [14–16] succeeds in describing the behaviour of polymer/colloid systems; a summary is given by Cohen [9]. Loops and particularly tails [15, 16] of an adsorbed polymer chain can extend into solution beyond the range of Coulombic repulsion of charged colloids (the Debye length), and thus can form bridges by adsorbing on to polymer-free sites on neighbouring particles. On the other hand, when colloids are near maximum polymer coverage, steric stabilization results [8].

Fundamental studies of the effects of adsorbed polymer on flocculation have been carried out using polymer solutions with a well-characterized, constant polymer molecular weight. However, in the polymerization-induced colloid aggregation (PICA) method the molecular weight and concentration of polymer changes with time as the acid-catalysed polymerization of urea and formaldehyde proceeds. In such a batch reaction, even in the absence of colloids, urea–formaldehyde (UF) polymer beads of narrow size distribution can be formed. With ZrO_2 sol present, composite spheres of narrow size distribution that consist of UF polymer and ZrO_2 colloids are formed.

We have already reported the effects of several processing variables for the aggregation of 70 nm ZrO_2 colloids [17]. This work suggested that one means of controlling the aggregation process and the porosity was to regulate the rate of polymer growth. A convenient way to do this is by adjusting the reaction pH.

‡ Author to whom all correspondence should be addressed.

0022–2461

This work reports and discusses the dramatic effect of initial sol pH on the synthesis process, on the apparent density, zirconia content, ZrO_2 yield, particle-formation time and pore structure. These changes are explained qualitatively in terms of the rate of polymer growth.

2. Experimental procedure

Aqueous zirconia sol (pH = 3.0), containing 20 wt % ZrO_2 particles, was purchased from Nyacol Products, Inc. (Ashland, MA). The particle-size distribution of the ZrO_2 colloids was determined by photon correlation analysis with a Coulter N4SD particle-size analyser using deionized water as the solvent. The reported weight per cent particle-size distribution is the average result of four analyses using a refractive index of 1.19 for the calculation. Urea (Mallinckrodt Specialty Chemical Co.), 37 wt % formaldehyde in water and methanol (Fisher Scientific) and concentrated nitric acid (EM Science) were also used.

The porous zirconia samples used in this study were synthesized by the following procedure: 100 ml ZrO_2 sol was added to a new 800 ml polypropylene beaker and the pH was adjusted to the desired value using concentrated nitric acid. 7.5 g urea was dissolved in the sol. With rapid mixing, 12.5 ml 37 wt % formaldehyde solution was added and the mixing was continued for an additional 30 s. After 2 h reaction, the sample was diluted to 700 ml total volume using deionized water and then homogenized by manual mixing. As noted previously for the preparation of porous zirconia [17] and silica [5, 18] by this method, there are two size-classes of aggregates which form: micrometre and submicrometre. The micrometre-scale aggregates of colloids were separated by sedimentation, resuspended in 2-propanol and collected by vacuum filtration; the resulting free-flowing powder was further dried at 90 °C in a convection oven for 12 h partially to remove adsorbed 2-propanol and water. A staged heating process was then used to remove the polymer and sinter the aggregates. The particles were first heated in a vacuum oven at 170 °C for 16 h and then at 375 °C for 2 h in a muffle furnace with sufficient air access to allow most of the carbon in the particles to be burned off. The temperature was raised to 750 °C for a further 6 h to burn off completely the carbon, and finally the particles were sintered at 900 °C for 3 h to improve their mechanical strength.

The apparent density of the composite and sintered (polymer-free) particles was measured by weighing a volumetric flask before and after loading the sample. The sample was loaded in a minimum of four increments; after each, the flask was tapped for at least 30 s to assist in uniform packing of the particles. Each sample was allowed to equilibrate with ambient air for 6 h before the determination of apparent density, to ensure a constant degree of hydration during the measurements.

The reaction time necessary for urea–formaldehyde polymer beads to form in the absence of ZrO_2 colloids was determined by monitoring the absorbance of a reaction mixture with the same concentrations of urea and formaldehyde as in a typical synthesis experiment. The reaction mixture was prepared by (1) dissolving urea in aqueous nitric acid of desired pH, (2) adding formaldehyde and (3) quickly homogenizing. It was then transferred to a cuvette and placed in a Bausch and Lomb Spectronic 88 spectrophotometer (λ = 500 nm) connected to a computer that collected the absorbance signal as a voltage every 2 s. The time at which particles formed in the presence of ZrO_2 sol was determined by viewing samples of the reaction mixture under a microscope. Changes in absorbance could not be used to determine the time of particle formation in this case because the ZrO_2 sol is opaque.

The weight per cent of ZrO_2 in the particles before polymer removal was determined by thermogravimetric analysis in flowing air or nitrogen using a Perkin–Elmer TGA7 instrument.

Nitrogen adsorption isotherms were collected at 77 K on a Porous Materials Inc. (Ithaca, NY) Automated BET Sorptometer. Scanning electron micrographs were taken with a Hitachi 450 scanning electron microscope.

Polymer adsorption data were collected by withdrawing 5 ml samples from standard reaction mixtures and diluting to 45 ml with deionized water. The samples were centrifuged for 10 min, the supernatant liquids were decanted and the precipitates were dried at 110 °C for 1 h. The weight per cent of polymer in the samples was determined by recording the weight of each sample before and after heating in a muffle furnace at 900 °C for 1 h.

3. Results

3.1. pH dependence of particle mechanical strength

The ZrO_2 colloid size distribution is shown in Fig. 1; the mean diameter is near 100 nm. Aggregates were prepared at pH values between 3.0 (the original sol pH) and 0.8. TGA traces were collected to quantify the weight per cent of water, urea–formaldehyde polymer and ZrO_2 in each sample. A representative TGA trace for a composite sample prepared at pH = 2.0 is shown in Fig. 2. Near pH = 1.5 the ZrO_2 content (Fig. 3a) goes through a maximum and the weight per cent of polymer (Fig. 3b) goes through a minimum. When the sol pH is higher than 1.4 the resulting sintered particles have adequate mechanical stability to withstand packing into HPLC columns at 5500 p.s.i. (10^3 p.s.i. = 6.89 N mm^{-2}) but when the sol pH is 1.4 or lower, the resulting particles cannot withstand column packing. For example, Fig. 4 shows the flow rates of a dispersing solvent (2-propanol) for particles synthesized at pH = 1.2 and 3.0. The consistently lower solvent flow rates for particles synthesized at pH = 1.2 demonstrate column plugging by fines formed from broken particles. The materials from the pH = 1.2 sol also provide very poor column efficiency, showing highly distorted elution peaks.

Fig. 5 shows a micrograph of particles prepared at pH = 0.8; they appear to be composed of very loosely packed submicrometre aggregates. Fig. 6 shows a

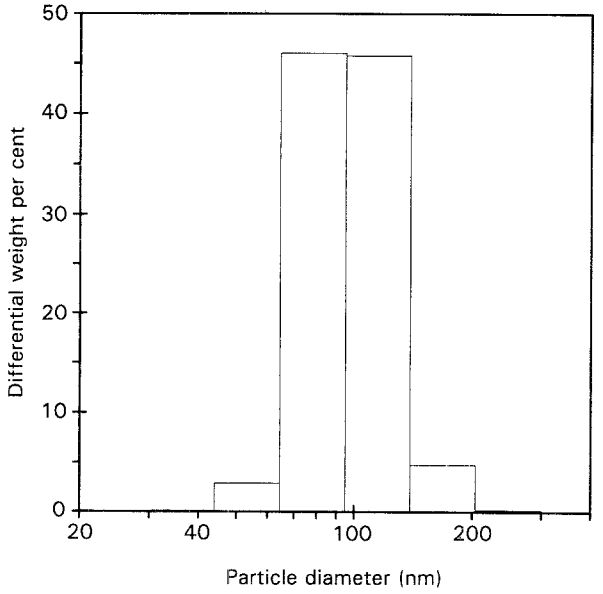

Figure 1 Zirconia colloid size distribution.

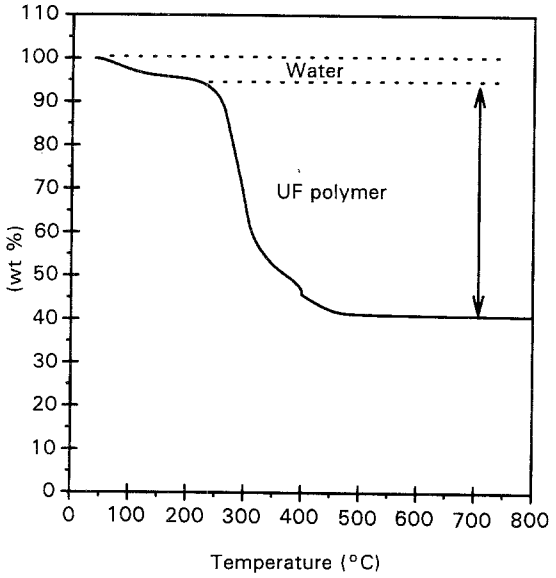

Figure 2 A TGA trace for ZrO_2 particles (before polymer removal) prepared using pH = 2.0 sol.

micrograph of a sintered sample that was synthesized at pH = 1.2. It is apparent that some particles are hollow spheres. Particles synthesized at pH = 1.4 also cannot withstand packing in an HPLC column at 5500 p.s.i., although no broken shells were observed by SEM. In contrast, a scanning electron micrograph of a sintered sample synthesized at pH = 3 (Fig. 7) shows no broken shells and can easily be packed in an HPLC column at 5500 p.s.i.

3.2. pH dependence of apparent density, composition and yield

The plot of apparent density of the composite aggregates, $\rho_{app,comp}$ (Fig. 3c) is in good agreement with the weight per cent of ZrO_2 in the particles determined by TGA (Fig. 3a). This verifies the existence of the maximum and confirms that the apparent density measurements are representative of particle density. The

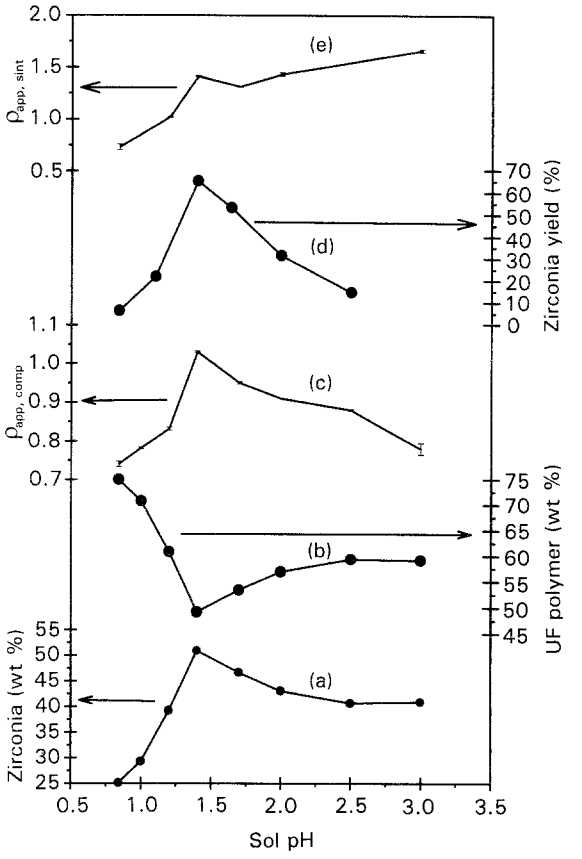

Figure 3 As a function of sol pH: (a) weight per cent of ZrO_2, (b) weight per cent of urea–formaldehyde polymer and (c) apparent density of the micrometre-scale particles before polymer removal ($g\,cm^{-3}$); (d) yield and (e) apparent density of sintered, micrometre-scale particles ($g\,cm^{-3}$). The weight per cent data correspond to dehydrated samples.

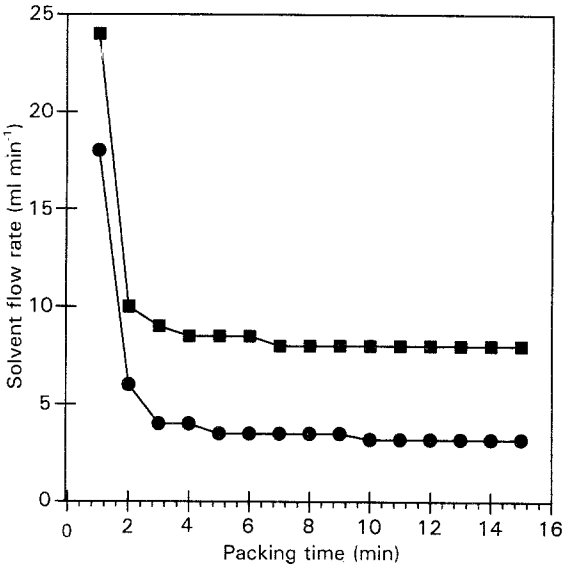

Figure 4 Packing-solvent flow rate profiles for particles synthesized using pH (■) 3.0 and (●) 1.2 sols. For both samples the packing apparatus, the column length (5 cm) and the ZrO_2 concentration in the slurry were the same and the packing pressure was 5000 p.s.i.

yield of micrometre-scale, sintered ZrO_2 particles (Fig. 3d) also goes through a maximum near pH = 1.5. The apparent density of sintered particles, $\rho_{app,sint}$, is shown in Fig. 3e; above pH = 1.4 we have found that the apparent density is very similar to that

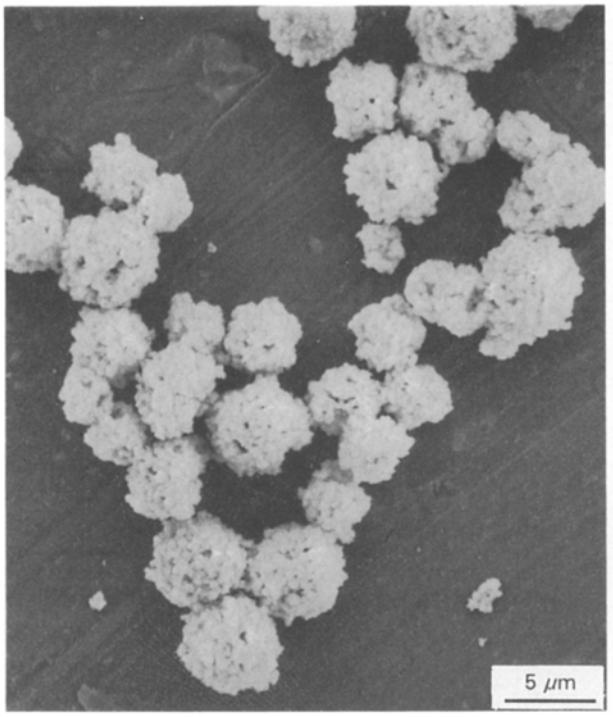

Figure 5 A scanning electron micrograph of sintered, porous ZrO_2 particles synthesized at pH = 0.8.

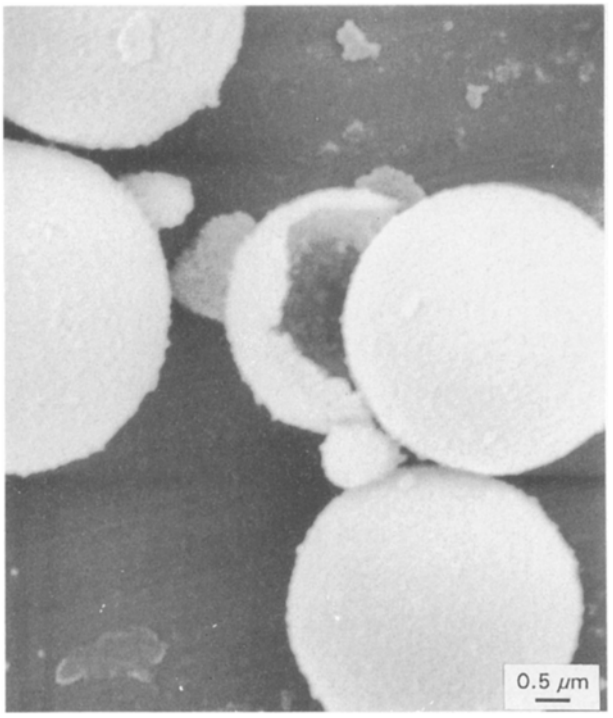

Figure 6 A scanning electron micrograph of sintered, porous ZrO_2 particles synthesized at pH = 1.2.

obtained by packing a HPLC column at high pressure with 2-propanol as the dispersing solvent. Below pH $\approx$ 1.4 there is a dramatic drop in apparent density of sintered particles, which is consistent with scanning electron micrographs of particles synthesized at pH = 0.8 (Fig. 5) and pH = 1.2 (Fig. 6).

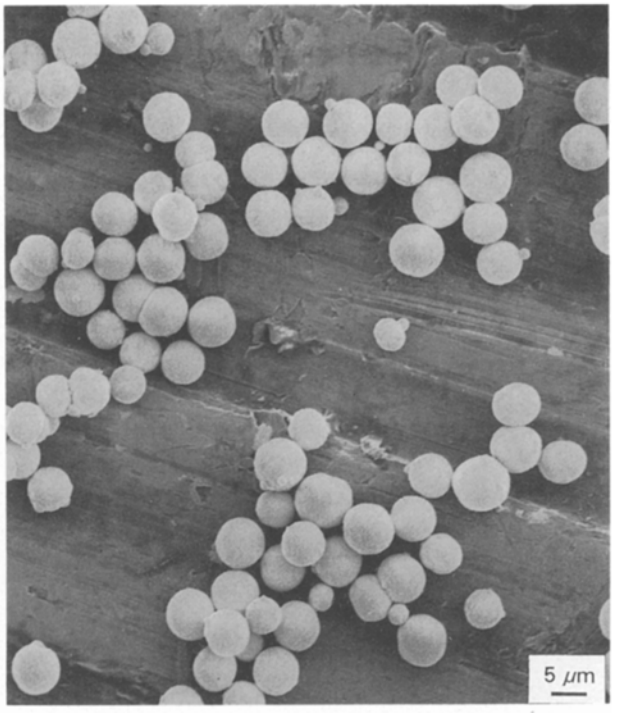

Figure 7 A scanning electron micrograph of sintered, porous ZrO_2 particles synthesized at pH = 3.

3.3. pH dependence of particle formation and polymer adsorption

The time of particle appearance during the polymerization of urea and formaldehyde, in both the presence and absence of ZrO_2 sol, is shown in Fig. 8. That both particle formation rates change in the same manner with pH suggests that the aggregate growth is governed by polymerization kinetics. Below pH $\sim$ 1.5, the ZrO_2/polymer particle formation rate is similar to that of the polymer alone. Above pH $\sim$ 1.5, though, the rate of ZrO_2/polymer particle formation diverges from the rate of precipitation of polymer alone. The faster appearance of the composite particles will be discussed below.

Fig. 9 shows the weight per cent of UF polymer in the composite particles collected by centrifugation using a range of pH. The weight per cent of polymer in the particles continues to increase long after particles are first observed in the microscope (Fig. 8), indicating that there must be a concentration gradient of UF polymer in the particles; this may influence the pore structure after the polymer is removed. While there is good qualitative agreement between Figs 9 and 3b, at all pH values the weight per cent of polymer after 400 min reaction in Fig. 9 is somewhat lower than in Fig. 3b. This is probably due to differences in the methods of sample collection. The data in Fig. 3 are for the micrometre-scale particles which are separated from the reaction mixture by repeated sedimentation-decanting sequences, whereas the data in Fig. 9 are for samples collected by centrifugation, and so will contain ZrO_2/polymer particles as well as some unreacted colloid. The unreacted colloid will serve to lower the measured weight per cent of polymer in the sample.

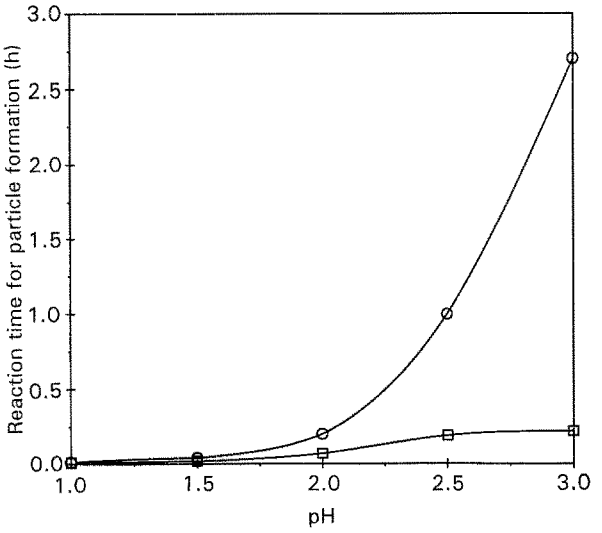

Figure 8 The time of (○) UF polymer bead formation and (□) ZrO_2 UF spherule appearance as a function of pH.

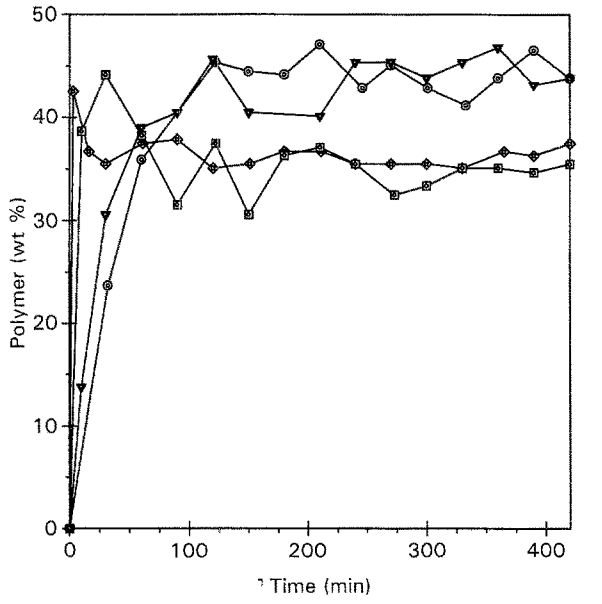

Figure 9 Adsorption of polymer on to ZrO_2 colloids at pH (⊙) 3, (▼) 2, (⊡) 1.4 and (◈) 1.2 as a function of reaction time.

3.4. Pore characterization

The pore-size distributions (psds) after sintering are shown in Fig. 10. All samples exhibit multimodal psds with pore diameters ranging between 10 and 45 nm. The sample synthesized at pH = 1.2 contains some hollow particles but its psd seems qualitatively similar to those of samples synthesized at higher pH (non-hollow particles). This is because nitrogen adsorption only probes the pores within the ZrO_2 shells and not the large voids they encompass. Surface areas and porosities, $\varepsilon_{particle}$, for these samples are listed in Table I. Note that there is qualitative agreement with Fig. 3e, but quantitative agreement is not expected, because condensing nitrogen cannot be used to distinguish between hollow cores and interstitial volume between aggregates. The nitrogen psds show that the higher the pH, the greater is the contribution of small pores to the total porosity.

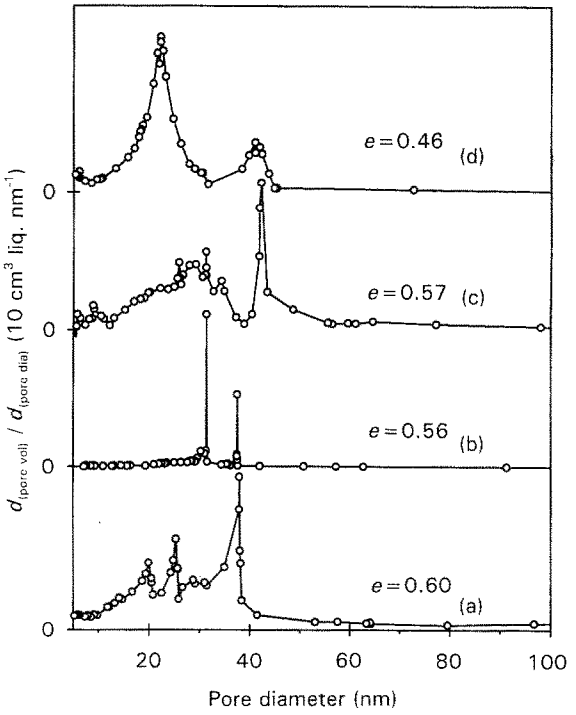

Figure 10 Pore-size distributions after sintering from nitrogen adsorption for particles synthesized at various pH: (a) 1.2, (b) 1.4, (c) 2.0 and (d) 3.0.

TABLE I Pore characterization data as a function of sol pH

Sol pH	Fractional particle porosity, $\varepsilon_{particle}$	Surface area ($m^2 g^{-1}$)	Fractional bed porosity, ε_{bed}
1.2	0.60	27	–
1.4	0.56	36	0.44
2.0	0.57	30	0.48
3.0	0.46	28	0.46

The porosity of the bed of particles, ε_{bed}, formed during apparent-density measurements for non-hollow particles (pH = 3, 2 and 1.4) can be calculated according to the equation

$$(1 - \varepsilon_{bed}) = \frac{\rho_{app,sint}}{(\rho_{ZrO_2})(1 - \varepsilon_{particle})} \quad (1)$$

where $\rho_{ZrO_2} = 5.7\ g\,cm^{-3}$; values of $\varepsilon_{particle}$ are listed in Table I and $\rho_{app,sint}$ is shown in Fig. 3e. The resulting bed porosities are included in Table I. The values are all similar so it is assumed that the particle packing density during apparent-density measurements is the same for each sample. Therefore, the apparent-density results reported here are proportional to the particle density. The bed porosity for hollow particles cannot be calculated by this method because $\varepsilon_{particle}$ is not accurately known (*vide supra*).

4. Discussion

4.1. pH dependence of polymerization and adsorption rates

Features of the particle-formation process can be interpreted in terms of urea–formaldehyde polymerization and polymer adsorption on ZrO_2 colloids. The

rate of urea–formaldehyde polymerization increases as the pH decreases (for pH $\leqslant$ 7.0) [19]. The rate of polymer adsorption is not appreciably sensitive to pH over the range studied because the entire range is on the acidic side of the isoelectric point for ZrO_2, and even if the surface charge was important, one would expect that the rate of polymer adsorption would decrease with decreasing pH. Instead, Figs 8 and 9 are consistent with the known trend that as pH increases the rate of UF polymerization decreases.

4.2. Influence of pH on reactive polymer-induced aggregation

There is a vast amount of evidence reported in the literature for the bridging flocculation of colloids with adsorbed polymers [7–16]. Although aggregation induced by neutralization of charged colloids by polyelectrolytes is well known [10], the urea–formaldehyde is uncharged. For non-reacting polymers, polymer-induced bridging flocculation is inhibited at high colloid-surface coverages [8]. In PICA, however, even if the colloids are fully covered by polymer, aggregation can occur because polymer bridges can form by further polymerization of the loops and tails of adsorbed polymer. A similar mechanism has been proposed for the "coacervation" of gelatine with low concentrations of resorcinol [20] in which a resorcinol molecule joins together by adsorption, loops and tails of gelatine macromolecules.

Between 2.5 $\leqslant$ pH $\leqslant$ 3.0, the time of composite particle (ZrO_2/UF) appearance increases by a factor of only 1.1, while that for UF polymer-bead formation increases by a factor of 2.7. In this pH range, polymerization is slow, so the concentration of polymer in solution is low. Fig. 9 shows the weight per cent of adsorbed polymer on ZrO_2 colloids during reaction at pH = 3. Aggregates are observed in the microscope after 15 min reaction, yet the weight per cent polymer on these aggregates is only a small fraction of the final coverage after 4 h reaction. At low polymer coverages, the hydrodynamic layer thickness is nearly independent of the molecular weight of the adsorbing polymer, but is a strong function of the amount of adsorbed polymer [9]. The hydrodynamic layer thickness should be small due to low surface coverage and, thus, aggregation should be slow. Presumably, then, the formation of polymer bridges between colloids is the rate-limiting step for particle formation. The weight per cent of polymer in the ZrO_2/polymer solid increases with reaction time because the molecular weight of the adsorbing polymer is increasing.

As the pH is decreased from 2.5 to $\sim$ 1.4, the rate of polymer growth increases. Therefore, there is less time for polymer adsorption on colloids before aggregation, so a continual decrease in the polymer content of the composite particles is observed. However, while fewer polymer segments adsorb on to the colloids before aggregation, the molecular weight of the adsorbed polymer is larger. The time of composite particle appearance decreases because the increasingly larger loops and tails of adsorbed polymer may extend further out into solution, escalating the probability of interaction and linkage formation with other colloids [8–13].

Below pH $\approx$ 1.5, the rate of polymer growth is high enough that, even before adsorption occurs, polymer beads are able to nucleate. Later, polymer-covered colloids connect with these beads to form a shell. As the pH decreases, the weight per cent of zirconia in the composite particles is approaching that in the reaction mixture ($\sim$ 20 wt %). This suggests that the mechanism of ZrO_2 incorporation in the composites resembles a physical entrapment process in which polymer adsorption is diminishingly important.

The optimum synthesis pH is, in principle, that which provides sufficient coverage of the ZrO_2 surface by urea–formaldehyde polymer necessary to connect the colloids and establish open pores while avoiding polymer nucleation. This pH also maximizes the number of polymer molecules available for the formation and growth of additional particles and it appears that this occurs at pH $\approx$ 1.5. The ZrO_2 content of the particles before polymer removal, and consequently the apparent density, go through maxima; so does the yield of sintered ZrO_2 particles. Conversely, the polymer content goes through a minimum (maximizing the yield of ZrO_2). Similarly, it has been shown that for non-reacting polymers, the aggregation efficiency goes through a maximum with colloid-surface coverage [8–11, 13, 16].

4.3. Colloid packing structure and particle mechanical strength

The aggregation process is very sensitive to the rate of polymerization and the amount of adsorbing polymer, as discussed above. It has also been shown that the rate of addition of polymer to a latex sol affects how aggregation proceeds with time [10]. It is clear from Fig. 3 that the rate of polymerization plays a significant role in the properties of the composite and sintered particles. It is interesting to compare the apparent density of the composite and sintered particles. On either side of pH $\approx$ 1.5 the polymer content of the composite particles increases, so the apparent density decreases because ZrO_2 is more dense than UF polymer. However, upon sintering, the apparent density increases monotonically with pH. Therefore, the degree of particle shrinkage must also change differently on either side of the optimum pH.

Shrinkage or sinterability of the aggregates is dependent upon both the colloid packing structure [21–24] and polymer content of the composites. The degree of shrinkage during sintering can be calculated from a mass balance using the data in Fig. 3, assuming that the bed porosity during measurement of apparent density was the same for all samples (Section 3.4). The bed porosities calculated from the experimental data are listed in Table I for the non-hollow particles. Because these values are all similar they are assumed to be the same for calculation of the shrinkage factor (d_{comp}/d_{sint} particle). However, the range of bed porosities was used to calculate the error bars on shrinkage factors. The shrinkage factor is calculated using the

following equations

$$\rho_{app,sint} = (\rho_{ZrO_2})(1 - \varepsilon_{particle})(1 - \varepsilon_{bed}) \quad (2)$$

$$(\rho_{app,comp})(\text{wt \% } ZrO_2)_{comp} = (\rho_{ZrO_2})(1 - \varepsilon_{particle})(1 - \varepsilon_{bed}) \quad (3)$$

For the composite particles, we will use the definition: $\varepsilon_{particle}$ = (non-ZrO_2 intraparticle volume)/(total particle volume). Assuming the density of dense ZrO_2 does not change, conservation of mass dictates that the volume of ZrO_2 in the particle remains constant during polymer removal and sintering. The shrinkage factor can then be calculated from the ratio of Equations 2 and 3, and noting that $(1 - \varepsilon_{particle})$ = (the volume of ZrO_2 in the particle)/(total particle volume)

$$\left[\frac{\rho_{app,sint}}{(\rho_{app,comp})(\text{wt\%}ZrO_2)_{comp}}\right]^{1/3} = \frac{d_{comp}}{d_{sint}} = \text{shrinkage factor} \quad (4)$$

The resulting data are shown in Fig. 11. Qualitatively, variation of the shrinkage factor and weight per cent of polymer in the composites (Fig. 3b) with pH is similar. Shrinkage due to polymer removal alone cannot explain the shrinkage factor results. The variation in the shrinkage factor with pH also reflects the vastly different colloid packing structures that form under different aggregation conditions. The minimum shrinkage near pH $\approx$ 1.5 indicates that the packing structure formed at this pH is very stable. Lange has addressed pore shrinkage during sintering in terms of the pore coordination number, R, which is the defined as the number of touching particles forming a pore [23]. Pore shrinkage will be greater in pores where R is less than a critical pore coordination number, R_c, than in pores where $R > R_c$; R_c is related to the ratio of the surface energy per unit area of grain boundaries and particle surfaces. Because sintering results in densification of the particles, there must also be concomitant particle shrinkage. Based on the work of Lange, near the optimum pH the colloid packing structure must consist of pores that have higher coordination numbers than those formed on either side of the optimum pH.

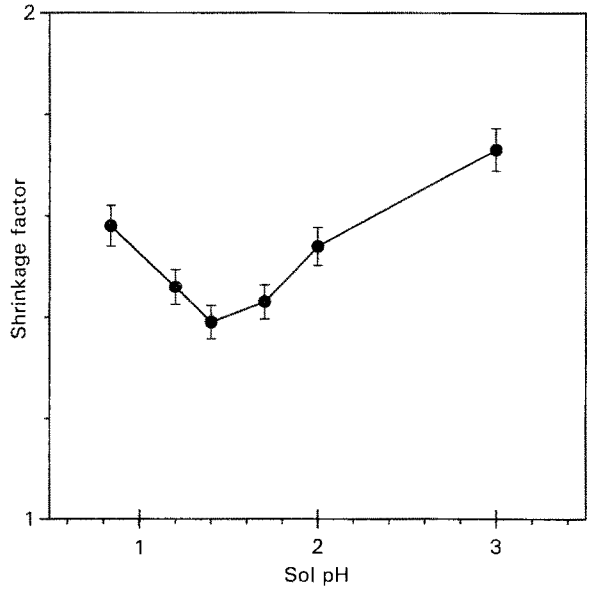

Figure 11 Shrinkage factors calculated as a function of pH: (shrinkage factor = d_{comp}/d_{sint} particle).

Variation in the colloid packing structure of the sintered aggregates with pH is also reflected in the relative mechanical strength of these aggregates. Mechanical strength is evaluated qualitatively based on the ability of the particles to withstand the HPLC column-packing process at 5500 p.s.i. In going from pH = 3 to pH = 1.4 there is a gradual monotonic decrease in the apparent density of sintered particles, whereas below pH = 1.4 there is a dramatic drop. Particles synthesized at pH $\leqslant$ 1.4 cannot withstand packing in an HPLC column; during the packing process broken pieces of particles plug the column. This poor mechanical strength of particles arises from the fact that at least some of the particles are hollow spheres, as illustrated in Fig. 6. Similar phenomena are observed with clusters of gold, silica and polystyrene prepared under rapid (diffusion-limited) and slow (reaction-limited) aggregation conditions [25]. Lin *et al.* [25] show that the clusters formed under rapid coagulation have much more open structures than the clusters formed under slow coagulation. Thus, it is not surprising that very rapid colloid aggregation results in loose packings of colloids. While the pore-size distributions based on nitrogen adsorption shown in Fig. 10 are qualitatively similar, the maximum pore size in each material increases with pH. The corresponding porosities and surface areas in Table I indicate a trend towards decreasing porosity with increasing sol pH. For samples synthesized above pH = 1.4, there is a significant contribution of the total pore volume by pores less than 30 nm in diameter. The presence of these smaller pores indicate a sufficiently dense colloid packing structure that can withstand the HPLC column-packing process.

Qualitatively, these results can be applied to similar colloid-aggregation processes. However, the rate of polymer adsorption strongly depends on the available colloid surface area. As the colloid surface area increases, the rate of polymer adsorption on a mass basis also increases and the optimum pH will decrease. With the kinetics of the urea–formaldehyde polymerization and polymer adsorption it should be possible to model this synthesis system and predict the optimum reaction pH for aggregation of different colloids.

5. Conclusions

The effects of solution pH on aggregate structure can be interpreted in terms of the rate of polymer growth. For the aggregation of 100 nm ZrO_2 colloids, the optimum falls near pH = 1.5. Near this optimum value the weight per cent of polymer in the composite particles and the shrinkage factor go through minima. The weight per cent of ZrO_2 in the composite particles and the yield of sintered ZrO_2 go through maxima. These trends are consistent with a mechanism involving the formation of polymer bridges between col-

loids and show the utility of PICA for controlling the packing structure of colloids in spherical aggregates.

Acknowledgements

The authors gratefully acknowledge support of this work from the National Institute of Health and the National Science Foundation and from the University of Minnesota Institute of Advanced Studies in Bioprocess Technology. The authors thank Professor Michael Flickinger for useful discussions on the pore structure requirements for protein chromatography. M.J.A. thanks Francisco Lorenzano-Porras for collection of the nitrogen adsorption data on the pH = 1.2 sample and Elizabeth Johnson for assistance with the colloid aggregation experiments.

References

1. J. A. BLACKWELL and P. W. CARR, *J. Chromatogr.* **596** (1992) 27.
2. U. TRUDINGER, G. MULLER and K. K. UNGER, *ibid.* **535** (1990) 111.
3. P. W. CARR, E. F. FUNKENBUSCH, M. P. RIGNEY, P. L. COLEMAN, D. A. HANGGI and W. A. SCHAFER, US Pat. 5015 373 (1991).
4. M. J. WAX and R. K. GRASSELLI, EP Pat. 0490226 A1 (1991).
5. R. K. ILER and H. J. McQUESTON, US Pat. 4010242 (1977).
6. A. BLEIER and R. M. CANNON, *Mater. Res. Symp. Proc.* **73** (1986) 71.
7. T. W. HEALY and V. K. LA MER, *J. Phys. Chem.* **66** (1962) 1835.
8. G. J. FLEER, and J. M. H. M. SCHEUTJENS, *Croat. Chem. Acta* **60** (1987) 477.
9. M. A. C. STUART, *Polym. J.* **23** (1991) 669.
10. A. ELAISSARI and E. PEFFERKORN, *J. Colloid Interface Sci.* **141** (1991) 522.
11. K. MÜHLE, *Colloid Polym. Sci.* **263** (1985) 660.
12. F. LAFUMA, K. WONG and B. CABANE, *J. Colloid Interface Sci.* **143** (1991) 9.
13. F. CSEMPESZ and S. ROHRSETZER, *Colloids Surf.* **31** (1988) 215.
14. J. M. H. M. SCHEUTJENS and G. J. FLEER, *J. Phys. Chem.* **83** (1979) 1619.
15. *Idem, ibid.* **84** (1980) 178.
16. *Idem, Macromolecules* **18** (1985) 1882.
17. L. SUN, M. J. ANNEN, F. LORENZANO, P. W. CARR and A. V. McCORMICK, *J. Colloid Interface Sci.* **163** (1994) 464.
18. R. W. STOUT and H. J. LEIBU, EP Pat. Appl. 0341556 (1989).
19. J. I. DE JONG and J. DE JONGE, *Rec. Trav. Chim.* **53** (1953) 139.
20. H. G. B. DE JONG, in "Colloid Science", Vol. II, edited by H. R. Kruyt (Elsevier, New York, 1949) p. 253.
21. F. F. LANGE, *J. Am. Ceram. Soc.* **67** (1984) 83.
22. E. LINIGER and R. RAJ, *ibid.* **70** (1987) 843.
23. F. F. LANGE, *ibid.* **72** (1989) 3.
24. L. MONTANARO and A. NEGRO, *J. Mater. Sci.* **26** (1991) 4511.
25. M. Y. LIN, H. M. LINDSAY, D. A. WEITZ, R. C. BALL, R. KLEIN and P. MEAKIN, *Nature* **339** (1989) 360.

Received 7 January
and accepted 16 May 1994